

Behavioral responses to jamming and ‘phantom’ jamming stimuli in the weakly electric fish *Eigenmannia*

Bruce A. Carlson · Masashi Kawasaki

Received: 27 March 2007 / Revised: 23 May 2007 / Accepted: 25 May 2007 / Published online: 3 July 2007
© Springer-Verlag 2007

Abstract The jamming avoidance response (JAR) of the weakly electric fish *Eigenmannia* is characterized by upward or downward shifts in electric organ discharge (EOD) frequency that are elicited by particular combinations of sinusoidal amplitude modulation (AM) and differential phase modulation (DPM). However, non-jamming stimuli that consist of AM and/or DPM can elicit similar shifts in EOD frequency. We tested the hypothesis that these behavioral responses result from non-jamming stimuli being misperceived as jamming stimuli. Responses to non-jamming stimuli were similar to JARs as measured by modulation rate tuning, sensitivity, and temporal dynamics. There was a smooth transition between the magnitude of JARs and responses to stimuli with variable depths of AM or DPM, suggesting that frequency shifts in response to jamming and non-jamming stimuli represent different points along a continuum rather than categorically distinct behaviors. We also tested the hypothesis that non-jamming stimuli can elicit frequency shifts in natural contexts. Frequency decreases could be elicited by semi-natural AM stimuli, such as random AM, AM presented to a localized portion of the body surface, transient changes in amplitude, and movement of resistive objects through the electric field. We conclude that ‘phantom’ jamming stimuli can induce EOD frequency shifts in natural situations.

Keywords Electric organ discharge · Jamming avoidance response · Sensory integration · Perception · Illusion

Abbreviations

AM	Amplitude modulation
Df	Difference in frequency
DPM	Differential phase modulation
EOD	Electric organ discharge
JAR	Jamming avoidance response
PM	Phase modulation

Introduction

The weakly electric fish *Eigenmannia* emits a quasi-sinusoidal electric organ discharge (EOD) that is used for communication and active electrolocation (Hopkins 1972, 1974; Heiligenberg 1973; Hagedorn and Heiligenberg 1985; Carlson 2006). When two individuals with similar EOD frequencies meet, their active electrolocation abilities are impaired by mutual interference (Heiligenberg 1973), which both fish actively avoid by shifting their frequencies away from each other (Watanabe and Takeda 1963; Bullock et al. 1972a, b). This jamming avoidance response (JAR) represents a powerful model system for understanding the neuronal control of natural behavior, from the encoding of the sensory information required to perform the behavior to the actual motor output (Heiligenberg 1991).

To execute the JAR, a fish must determine the sign of the frequency difference (Df) between its own EOD and its neighbor’s EOD (Df = neighbor’s EOD frequency – own EOD frequency), which is achieved by analyzing the spatiotemporal pattern of interference that results from combining the two EODs (Fig. 1). This interference is characterized by sinusoidal amplitude modulation (AM)

B. A. Carlson (✉) · M. Kawasaki
Department of Biology, University of Virginia,
Gilmer Hall, P.O. Box 400328, Charlottesville,
VA 22904-4328, USA
e-mail: bc6s@virginia.edu; carlson.bruce@gmail.com

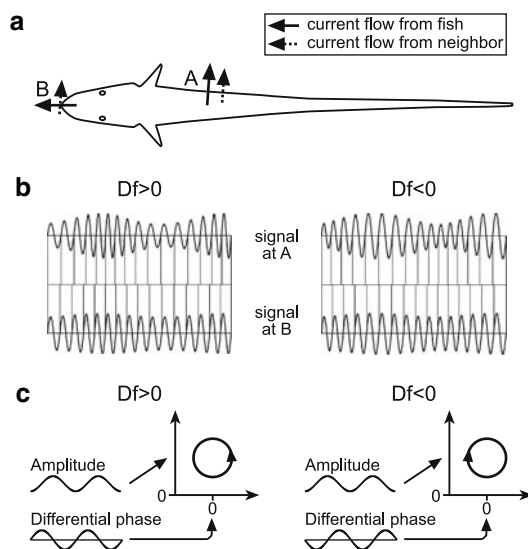


Fig. 1 Sensory cues for the JAR. **a** The different geometries of the fish's own EOD and its neighbor's EOD result in greater interference at the location marked A than at the location marked B. **b** Modulations in amplitude and phase for opposite signs of Df at locations A and B. The vertical lines mark the zero crossings of the signals at the two locations. **c** Amplitude at location A and difference in phase between locations A and B for opposite signs of Df . The temporal relationship between amplitude and differential phase is reversed when switching the sign of Df , which results in a different direction of rotation in a Lissajous graph

and phase modulation (PM). Although the rate of AM and PM is equal to the magnitude of Df , and is therefore identical for opposite signs of Df , the temporal relationship between AM and PM differs for opposite signs of Df . For $Df > 0$, PM is advanced by 90° relative to AM, but for $Df < 0$, PM is delayed by 90° relative to AM. In addition, the depth of modulation varies at different points along the body surface due to the different orientations of the two electric fields. By combining information about AM and differences in phase between different locations on the body surface (differential PM, or DPM), the fish is able to determine the sign of Df and shift its EOD frequency accordingly. If one plots the pattern of AM against the pattern of DPM as Lissajous graphs that develop over time, one obtains circular graphs that rotate in a counterclockwise direction with $Df > 0$ stimuli, and a clockwise direction with $Df < 0$ stimuli (Fig. 1c). It is this sense of rotation that the fish use to determine the sign of Df (Heiligenberg et al. 1978; Heiligenberg and Bastian 1980; Takizawa et al. 1999).

The AM and PM are largely encoded separately by two distinct populations of primary electrosensory afferents, amplitude-coding P-afferents, and time-coding T-afferents (Scheich et al. 1973; Zakon 1986). Plotting Lissajous graphs of the spike rates of P-afferents against the spike times of T-afferents results in circular graphs that show the

same sense of rotation as $Df > 0$ and $Df < 0$ stimuli (Fig. 2a, b), revealing that the primary afferents provide the necessary information for performing the JAR (Heiligenberg and Partridge 1981; Carlson and Kawasaki 2006). However, the spike times of T-afferents are slightly affected by AM, and the spike rates of P-afferents are slightly affected by PM (Carlson and Kawasaki 2006). This lack of independence in the encoding of AM and PM can therefore result in 'phantom' modulations in amplitude or phase that arise within the nervous system but are not actually present in the stimulus, as seen in Lissajous plots of the primary afferent responses to sinusoidal AM and sinusoidal DPM (Fig. 2a, b). The sense of rotation in Lissajous plots of primary afferent responses accurately predicts the direction of EOD frequency shifts, with clockwise rotations corresponding to frequency increases and counterclockwise rotations corresponding to frequency decreases (Fig. 2c). This indicates that the lack of independence in the encoding of AM and PM can ultimately cause fish to mistakenly perceive 'phantom' jamming stimuli (Carlson and Kawasaki 2006). We tested this hypothesis by making quantitative comparisons of behavioral responses (EOD frequency shifts) to a variety of jamming and non-jamming electrosensory stimuli. In addition, we tested the hypothesis that phantom jamming stimuli can elicit EOD frequency shifts in semi-natural situations.

Materials and methods

Animals

We used a total of 39 adult *Eigenmannia* sp., ranging in total length from 10.5 to 17.0 cm. Fish were purchased from commercial vendors and maintained in groups of 10–30 fish in aerated, filtered tanks, with the temperature set at 24–28°C, and the conductivity set at 100–200 $\mu\text{S}/\text{cm}$. The EOD frequency of each fish was measured before the start of an experiment, and ranged from 220 to 360 Hz. Fish were then immobilized and their EODs were attenuated by an intra-muscular injection of Flaxedil (gallamine triethiodide, 2.0 μl of a 3.0 mg/ml solution; Sigma, St. Louis, MO, USA). Fish were placed in a sponge-lined clamp that gently held them upright and completely immersed in water. Ventilation was provided by a stream of aerated water fed into the fish's mouth.

EOD frequency recording and response measurement

Although the electric organ is silenced by Flaxedil, the EOD command signal can still be recorded through a tail electrode that picks up the activity of the electromotor neurons that normally drive the electric organ. This signal

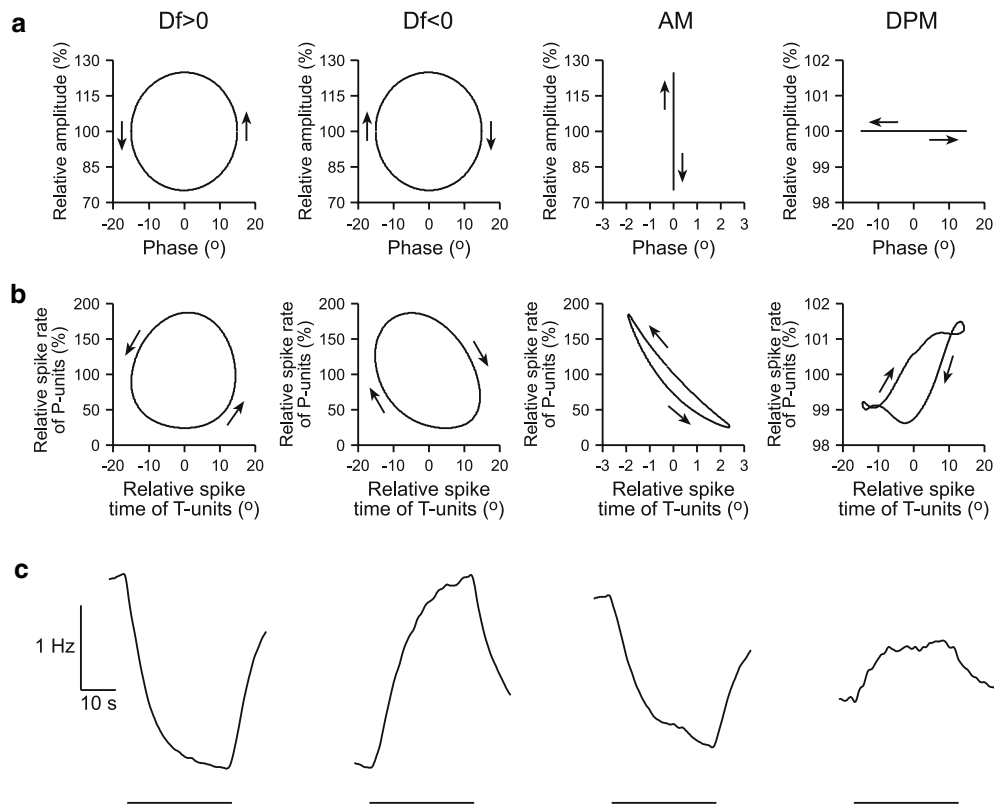


Fig. 2 Neural representations and behavioral responses to sinusoidal stimulus modulations. **a** Sinusoidal stimulus modulations plotted as Lissajous graphs of relative amplitude versus phase. **b** Primary afferent responses to the stimuli in **(a)** plotted as Lissajous graphs of the mean relative spike rate of P-afferents ($n = 33$ units) versus the mean relative spike time of T-afferents ($n = 16$ units). Data are taken from Carlson and Kawasaki (2006). Note that in both **(a)** and **(b)**, the

abscissa is magnified for AM and the ordinate is magnified for DPM to better illustrate the sense of rotation in the neural representations. **c** Changes in EOD frequency in a single individual in response to the stimuli in **(a)** presented using the phase chamber configuration. The average responses to three repeated presentations of each stimulus are shown, and the *bar* beneath each average response represents the period of stimulus modulation

was amplified 1,000× by a differential A/C amplifier then fed into a Schmitt trigger that generated a 5 V TTL pulse at the start of each EOD cycle. The output of the Schmitt trigger was fed into a divide-by-ten counter that was output to an event timer with a clock rate of 1 MHz (Tucker–Davis Technologies model ET1, Gainesville, FL, USA). The time-stamped pulses were then converted into average EOD frequencies at a sampling rate of 4 Hz (average EOD frequency was calculated every 250 ms) and the resulting values were saved to disk using custom-made software for Matlab 7.0.1 (The Mathworks Inc., Natick, MA, USA).

Traditionally, the magnitude of JARs has been expressed as the magnitude of EOD frequency changes in response to alternating presentation of $Df > 0$ and $Df < 0$ (Heiligenberg 1991). However, this approach only provides a differential measure of responses to opposite signs of Df , and not the actual characteristics of responses to particular stimuli relative to baseline (Bastian and Yuthas 1984; Takizawa et al. 1999). Because we were interested in separately quantifying the responses to $Df > 0$, $Df < 0$, and non-jamming stimuli, we presented all stimuli from a

baseline of no stimulus modulation for a duration of 30 s. The magnitude of frequency shifts was determined as the mean value of the EOD frequency relative to baseline over the entire period of stimulation, divided by the duration of stimulation (Hz/min). This value was then averaged from three repeated presentations of each stimulus. All statistical analyses were done using Statistica 6.1 (StatSoft Inc., Tulsa, OK, USA).

Electrosensory stimulation

All electric stimuli were numerically generated using custom-made software for Matlab 7.0.1 according to:

$$V(t) = A_c [1 + s_{AM}(t)] \sin(2\pi f_c t - s_{PM}(t)),$$

where $V(t)$ is the stimulus voltage at time t , A_c the carrier amplitude, f_c the carrier frequency, and $s_{AM}(t)$ and $s_{PM}(t)$ are time-varying modulations in amplitude and phase, respectively. Stimuli were delivered via a digital-to-analog converter at a sampling rate of 20 kHz (Tucker–Davis

Technologies model DA3-4). Two programmable attenuators (Tucker–Davis Technologies model PA4) were used to adjust the stimulus amplitude and the resulting signals were delivered using homemade isolators with field effect transistors.

We used four different experimental set-ups (Fig. 3). In three of these conditions ('global,' 'local,' and 'object motion'), we provided a substitute EOD replacement designed to mimic the fish's own EOD by placing an anodal electrode in the fish's mouth and a cathodal electrode just behind the fish's tail ('EOD replacement' in Fig. 3a–c). A sinusoidal electric field was constantly played through this electrode pair, with the carrier frequency set to within 5 Hz of the fish's EOD frequency as measured before the injection of Flaxedil and the carrier amplitude set at 1–3 mV/cm as measured near the gill covers.

In the 'global' stimulus configuration (Fig. 3a), a second sinusoidal electric field designed to mimic a natural, tangential electric field from a neighbor was provided via a pair of electrodes placed on opposite sides of the fish ('global stimulus' in Fig. 3a) (Chacron et al. 2003). To

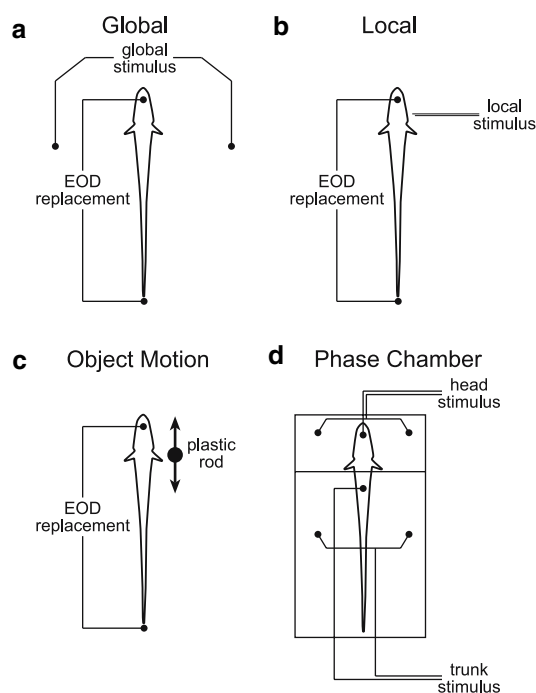


Fig. 3 Stimulus configurations. **a** In the 'global' configuration, the fish is provided with an EOD replacement and jamming stimuli are presented by a pair of electrodes oriented perpendicular to the long axis of the fish. **b** In the 'local' configuration, the fish is provided with an EOD replacement and stimuli are presented by a fine pair of electrodes placed near the fish's head. **c** In the 'object motion' configuration, the fish is provided with an EOD replacement and a plastic rod moves along the side of the fish. **d** In the 'phase chamber' configuration, the fish is divided into electrically isolated 'head' and 'trunk' compartments that receive independent electrical stimulation

characterize tuning to modulation rate, we presented jamming stimuli through the global stimulus electrodes at 12 different carrier frequencies, including $\pm 1, 2, 4, 8, 16,$ and 32 Hz relative to the EOD replacement frequency. The carrier amplitudes of these jamming stimuli were adjusted to generate an AM depth of 15–20%, and this amplitude was held constant for all 12 stimuli presented to a given fish.

We also presented fish with global AM stimuli by modulating the amplitude of the EOD replacement (no stimulus delivered through the global stimulus electrodes). These stimuli included sinusoidal AM at rates of 1, 2, 4, 8, 16, and 32 Hz and a depth of 25% to characterize tuning to modulation rate, as well as sinusoidal AM at a rate of 4 Hz with depths ranging from 0.01 to 25%. We characterized responses to Gaussian distributed random AM with a SD of 25% and frequency components ranging from 0 to 20, 0 to 100, 30 to 100, 50 to 100, or 70 to 100 Hz, obtained through Butterworth low-pass or band-pass filtering. We also obtained responses to random AM with frequency components ranging from 0 to 20 Hz and SDs ranging from 0.01 to 25%. To assess responses to transient changes in amplitude, we measured responses to upward and downward linear ramps of 250 ms duration and amplitudes of 10, 25, and 50% of the carrier amplitude.

In the 'local' stimulus configuration (Fig. 3b), a second sinusoidal electric field was delivered to a restricted region just anterior to the gill cover via a small dipole pair of electrodes separated by 2 mm and oriented perpendicular to the fish (Bastian et al. 2002; Chacron et al. 2003). The carrier frequency and phase of this stimulus were identical to the EOD replacement, and the carrier amplitude at the site of stimulation was adjusted to 50% of the carrier amplitude of the global replacement. Modulating the amplitude of the local stimulus therefore resulted in a local AM signal experienced by the fish with a depth equal to 50% of the depth being presented through the electrode pair. The amplitude of the local stimulus attenuated rapidly with distance, decreasing to $\sim 25\%$ of the source amplitude 1 cm away from the electrode pair, and decreasing to undetectable levels 2 cm away, as measured by a pair of dipoles spaced 2 mm apart. The local stimulus configuration therefore resulted in highly localized modulations in amplitude. We measured responses to sinusoidal AM at a rate of 4 Hz and random AM with frequency components ranging from 0 to 20 Hz, with SDs ranging from 0.01 to 25% in both cases.

We presented fish with moving resistive objects in the 'object motion' configuration (Fig. 3c) (Ramcharitar et al. 2005). A pen plotter was used to move a plastic rod back and forth along the side of the fish in a sinusoidal motion at a rate of 1 Hz. The most rostral extent of the object was

~1 cm past the tip of the snout and the total distance covered was ~5 cm (corresponds to an average rate of motion of ~10 cm/s). We used rods of three different diameters: 3, 5, and 6 mm. The length of the rods extended from above the surface of the water to ~2 cm below the ventral edge of the fish. Responses were also obtained in the absence of an EOD replacement as a control to verify that responses were mediated by the tuberous electrosensory system, rather than a different modality (e.g., mechanosensory lateral line, visual, or auditory).

To independently stimulate fish with AM and DPM, we used a ‘phase chamber’ to divide the fish into electrically isolated head and trunk compartments (Fig. 3d) (Heiligenberg and Bastian 1980). In this configuration, two independent EOD replacement signals were provided to the head and trunk. These signals had identical carrier frequencies, which were set to within 5 Hz of the fish’s EOD frequency as measured before the injection of Flaxedil. Stimuli to the head were provided through an anodal electrode placed in the mouth and two cathodal electrodes placed on either side of the fish’s head. Stimuli to the trunk were provided through an anodal pin electrode placed in the dorsal musculature and two cathodal electrodes placed on either side of the fish’s trunk. The carrier amplitudes of both signals were set to 1–3 mV/cm as measured near the skin surface.

Unless stated otherwise, all stimulus modulations in the phase chamber (sinusoidal AM, sinusoidal DPM, or a combination of both) were generated by modulating the signal in the head compartment while the signal in the trunk compartment remained unmodulated. We generated $Df > 0$ and $Df < 0$ stimuli by advancing or delaying sinusoidal DPM by 90° relative to sinusoidal AM, respectively, and except where noted, the depths of AM (AM_d , in %) and PM (PM_d , in degree) were set according to the relationship that occurs naturally with actual jamming stimuli:

$$AM_d = 100 \times \sin\left(\frac{PM_d \times \pi}{180}\right).$$

We obtained responses to sinusoidal AM, sinusoidal DPM, $Df > 0$, and $Df < 0$ at modulation rates of 1, 2, 4, 8, 16, and 32 Hz to characterize tuning to modulation rate (AM depth = 25% and PM depth = 14.4775° in each case).

To characterize sensitivity to sinusoidal AM, sinusoidal DPM, $Df > 0$, and $Df < 0$, we presented all four stimuli in the phase chamber at a modulation rate of 2 Hz, with AM depths ranging from 0.001 to 25% and PM depths ranging from 0.001 to 15° . We estimated the minimum modulation depth that would elicit a response by fitting the shift in EOD frequency against the depth of modulation using the following model:

$$y = \begin{cases} 0 & , \text{if } x < -b/m, \\ mx + b, & x \geq -b/m \end{cases},$$

where x is the logarithm of the modulation depth (in % for AM, or degrees for PM), y the shift in EOD frequency (in Hz/min), and m and b are the slope and y -intercept of a standard linear regression equation. This model therefore fits a linear regression to the relationship between x and y for all values of x greater than the x -intercept, and sets all values below the x -intercept equal to 0. We estimated the sensitivity from each fit as the value of the x -intercept (minimum depth that elicited a response), which is equal to $-b/m$.

We characterized the time course of responses to sinusoidal AM, sinusoidal DPM, $Df > 0$, and $Df < 0$ presented in the phase chamber following the method of Bastian and Yuthas (1984). First, we converted EOD frequencies into intervals and determined the maximum interval (for decreases in EOD frequency) or minimum interval (for increases in EOD frequency) during the response. We then calculated the time constant of the response as the duration from the start of the stimulus to the time when the EOD interval reached 63.21% of the maximum or minimum value. Finally, we evaluated a fit of the data to a simple exponential curve generated from the observed time constant and change in interval. We used the same method to evaluate exponential fits to stimuli presented in free-field conditions.

We also presented sinusoidal stimulus modulations in which the AM depth was held constant at 25%, while the PM depth was varied from 0 to 15° and the PM was advanced or delayed by 90° relative to AM (as in $Df > 0$ and $Df < 0$ conditions, respectively). Similarly, we presented sinusoidal stimulus modulations in which the PM depth was held constant at 15° , while the AM depth was varied from 0 to 25% and the PM was advanced or delayed by 90° relative to AM.

Results

Tuning to stimulus modulation rate

Under global stimulus conditions that mimic natural jamming stimuli (i.e., Fig. 3a), responses to $Df > 0$ were typically greatest at modulation rates of 2 or 4 Hz (Fig. 4a), whereas responses to $Df < 0$ were typically greatest at modulation rates of 1 or 2 Hz (Fig. 4b). $Df > 0$ responses were therefore tuned to higher rates of modulation than $Df < 0$ responses (sign test, $n = 18$, $z = 3.474$, and $P < 0.001$). Responses to AM were also tuned to higher rates of modulation, typically 4 Hz (Fig. 4c). We used

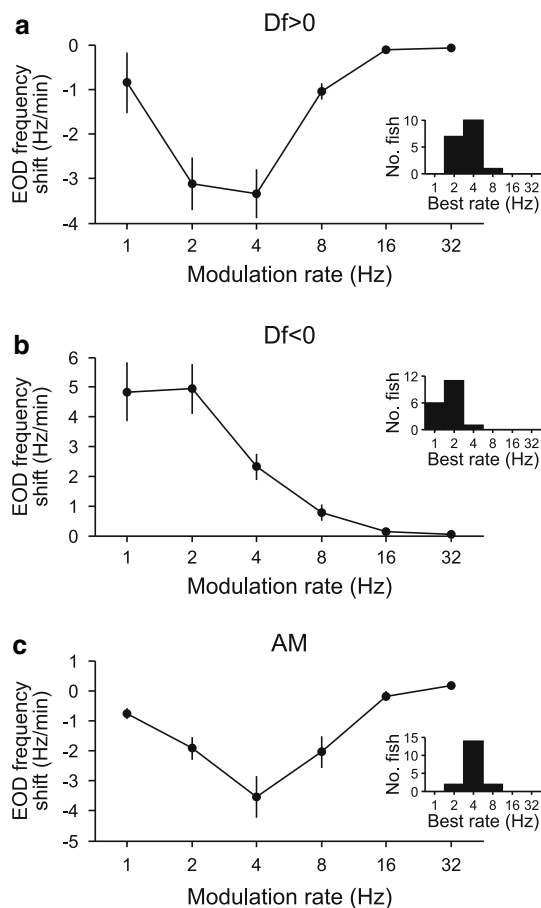


Fig. 4 Tuning to modulation rate in the global stimulus configuration for responses to Df>0 (**a**), Df<0 (**b**), and sinusoidal AM (**c**). Plots show the mean shift in EOD frequency (\pm SEM and $n = 18$ fish) as a function of modulation rate (1, 2, 4, 8, 16, and 32 Hz). Insets show the distribution of modulation rates that elicited the greatest shift in EOD frequency for each fish ('Best rate')

multiple regression to compare the average AM tuning curve with the average tuning curves to Df>0 and Df<0 ($r^2 = 0.8206$). Average AM responses to different rates of modulation were correlated with responses to Df>0 ($\beta = 1.040 \pm 0.300$, $t_3 = 3.467$, and $P < 0.05$), but not with responses to Df<0 ($\beta = 0.284 \pm 0.300$, $t_3 = 0.945$, and $P > 0.4$).

Similar differences in the tuning of responses to Df>0 and Df<0 were obtained when stimulation was provided through the phase chamber (i.e., Fig. 3d), for which Df>0 responses were tuned to higher rates of modulation than Df<0 responses (Fig. 5a, b; sign test, $n = 11$, $z = 2.667$, and $P < 0.01$). AM responses were tuned to higher rates of modulation (Fig. 5c), similar to Df>0 responses, whereas DPM responses were tuned to lower rates of modulation (Fig. 5d), similar to Df<0 responses. We used multiple regression to compare the average AM and DPM tuning curves with the average tuning curves to Df>0 and Df<0 ($r^2 = 0.9993$ for AM regression and $r^2 = 0.8366$ for DPM

regression). Average AM responses to different rates of modulation were strongly correlated with responses to Df>0 ($\beta = 1.078 \pm 0.023$, $t_3 = 47.58$, and $P < 0.0001$), but relatively weakly correlated with responses to Df<0 ($\beta = 0.113 \pm 0.023$, $t_3 = 4.988$, and $P < 0.05$). In contrast, average DPM responses to different rates of modulation were not correlated with responses to Df>0 ($\beta = 0.632 \pm 0.337$, $t_3 = 1.873$, and $P > 0.15$), but were correlated with responses to Df<0 ($\beta = 1.260 \pm 0.337$, $t_3 = 3.733$, and $P < 0.05$).

Sensitivity to modulation depth

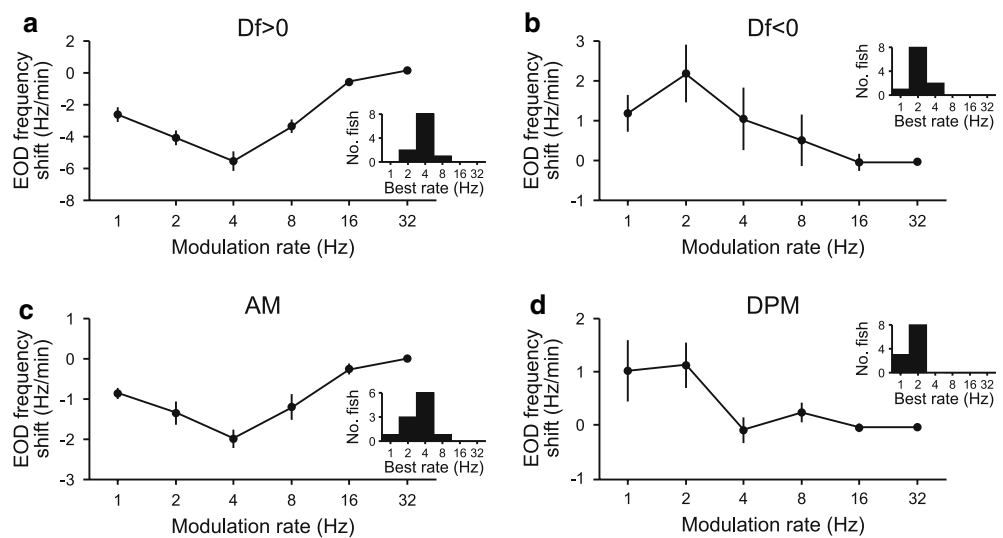
We quantified the sensitivity of 11 individual fish to Df>0, Df<0, sinusoidal AM, and sinusoidal DPM by presenting all four stimuli in the phase chamber (i.e., Fig. 3d) at a modulation rate of 2 Hz and several different depths of modulation. Figure 6a shows an example of the procedure we used to estimate sensitivity (see Methods). For Df>0, the average minimum depth that elicited a response was 0.2420% (ranging from 0.0322 to 1.5465%), or 0.1387° (ranging from 0.0185 to 0.8861°). For Df<0, the average minimum depth that elicited a response was 0.5412% (ranging from 0.0419 to 1.7955%), or 0.3100° (ranging from 0.0240 to 1.0288°). Therefore, the fish exhibited greater sensitivity to Df>0 than to Df<0 ($t_{10} = 2.518$ and $P < 0.05$).

The fish exhibited comparable sensitivity to AM, for which the average minimum depth that elicited a response was 0.2485% (ranging from 0.0274 to 1.1548%). However, the fish were relatively insensitive to DPM, for which the average minimum depth that elicited a response was 1.9064° (ranging from 0.8680 to 6.3334°). We used multiple regression to compare the minimum depths that elicited responses to sinusoidal AM and sinusoidal DPM with the minimum depths that elicited responses to Df>0 and Df<0 ($r^2 = 0.8113$ for AM regression and $r^2 = 0.5257$ for DPM regression). Sensitivity to AM (Fig. 6b) was strongly correlated with Df>0-sensitivity ($\beta = 0.918 \pm 0.158$, $t_8 = 5.798$, and $P < 0.001$), but not Df<0-sensitivity ($\beta = -0.086 \pm 0.158$, $t_8 = -0.541$, and $P > 0.60$). In contrast, sensitivity to DPM (Fig. 6c) was not correlated with Df>0-sensitivity ($\beta = -0.117 \pm 0.251$, $t_8 = -0.467$, and $P > 0.65$), but was correlated with Df<0-sensitivity ($\beta = 0.744 \pm 0.251$, $t_8 = 2.966$, and $P < 0.05$).

Time course of responses

Under free-field conditions (i.e., Fig. 3a), behavioral responses to jamming stimuli (Df = ± 2 Hz) were accurately fit by simple exponential curves (see Methods). For responses to Df>0, the mean r^2 -value (\pm SEM) was 0.9411 ± 0.0125 , and for responses to Df<0, it was

Fig. 5 Tuning to modulation rate in the phase chamber configuration for responses to $Df > 0$ (a), $Df < 0$ (b), sinusoidal AM (c), and sinusoidal DPM (d). Plots show the mean shift in EOD frequency (\pm SEM and $n = 11$ fish) as a function of modulation rate (1, 2, 4, 8, 16, and 32 Hz). Insets show the distribution of modulation rates that elicited the greatest shift in EOD frequency for each fish ('Best Rate')



0.9291 ± 0.0201 ($n = 18$ fish). On average, the time constant of responses to $Df > 0$ was longer than the time constant of responses to $Df < 0$ (10.0694 ± 0.8377 and 7.9861 ± 0.8988 s, respectively), but this difference was not significant ($t_{17} = 1.700$ and $P = 0.1$).

We examined the time course of the behavioral responses of 22 individual fish to $Df > 0$, $Df < 0$, sinusoidal AM, and sinusoidal DPM presented in the phase chamber (i.e., Fig. 3d) at a modulation rate of 2 Hz and an AM depth of 25% (PM depth = 14.4775°). Responses to all four stimuli were accurately fit by a simple exponential curve ($Df > 0$: $r^2 = 0.9780 \pm 0.0057$; $Df < 0$: $r^2 = 0.9226 \pm 0.0149$; AM: $r^2 = 0.9304 \pm 0.0137$; PM: $r^2 = 0.7904 \pm 0.0406$). As with the free-field conditions, there was no significant difference between the time constants of responses to $Df > 0$ and $Df < 0$ ($t_{21} = 0.899$ and $P = 0.37$). However, in analyzing differences across individuals, we found that variation in the time constant of $Df > 0$ responses tended to be correlated with variation in the time constant of AM responses, whereas variation in the time constant of $Df < 0$ responses tended to be correlated with variation in the time constant of DPM responses (Fig. 7). We used multiple regression to compare the time constants of responses to sinusoidal AM and sinusoidal DPM with the time constants of responses to $Df > 0$ and $Df < 0$ ($r^2 = 0.4035$ for AM regression and $r^2 = 0.2980$ for DPM regression). AM time constants were positively correlated with $Df > 0$ time constants ($\beta = 0.407 \pm 0.178$, $t_{19} = 2.289$, and $P < 0.05$), but negatively correlated with $Df < 0$ time constants ($\beta = -0.455 \pm 0.178$, $t_{19} = -2.562$, and $P < 0.05$). In contrast, DPM time constants were not significantly correlated with $Df > 0$ time constants ($\beta = 0.269 \pm 0.193$, $t_{19} = 1.394$, and $P > 0.15$), but were positively correlated with $Df < 0$ time constants ($\beta = 0.498 \pm 0.193$, $t_{19} = 2.581$, and $P < 0.05$).

Responses to variation in the relative depths of AM and PM

Using the phase chamber (i.e., Fig. 3d), we measured shifts in EOD frequency in response to stimuli with the same temporal relationship between AM and DPM that occurs with natural jamming stimuli (DPM advanced or delayed by 90° relative to AM for $Df > 0$ and $Df < 0$, respectively), but in which the relative depths of AM or PM were varied over a range of values. In one set of experiments, the AM depth was held constant at 25% while the PM depth was varied from 0 to 15° ($n = 10$ fish), and in the other set of experiments, the PM depth was held constant at 15° while the AM depth was varied from 0 to 25% ($n = 8$ fish). In both cases, we plotted the mean shift in EOD frequency as a function of either PM depth or AM depth, with negative and positive depths reflecting clockwise and counterclockwise rotations, respectively, in Lissajous plots of the stimulus modulations (Fig. 8).

The resulting plots clearly reveal two plateaus: accelerations in EOD frequency occurring in response to a counterclockwise rotation, decelerations occurring in response to a clockwise rotation, and an abrupt transition between the two. We fit the data with a sigmoidal function of the form:

$$y = \left(\frac{a}{1 + e^{-\left(\frac{x-b}{c}\right)}} \right) + d,$$

where a is the difference in height between the two plateaus, b the mid-point between the two plateaus along the x -axis, c the steepness, or slope, of the transition between the two plateaus, and d is the vertical offset of the curve. The fit of mean responses to variation in PM depth yielded

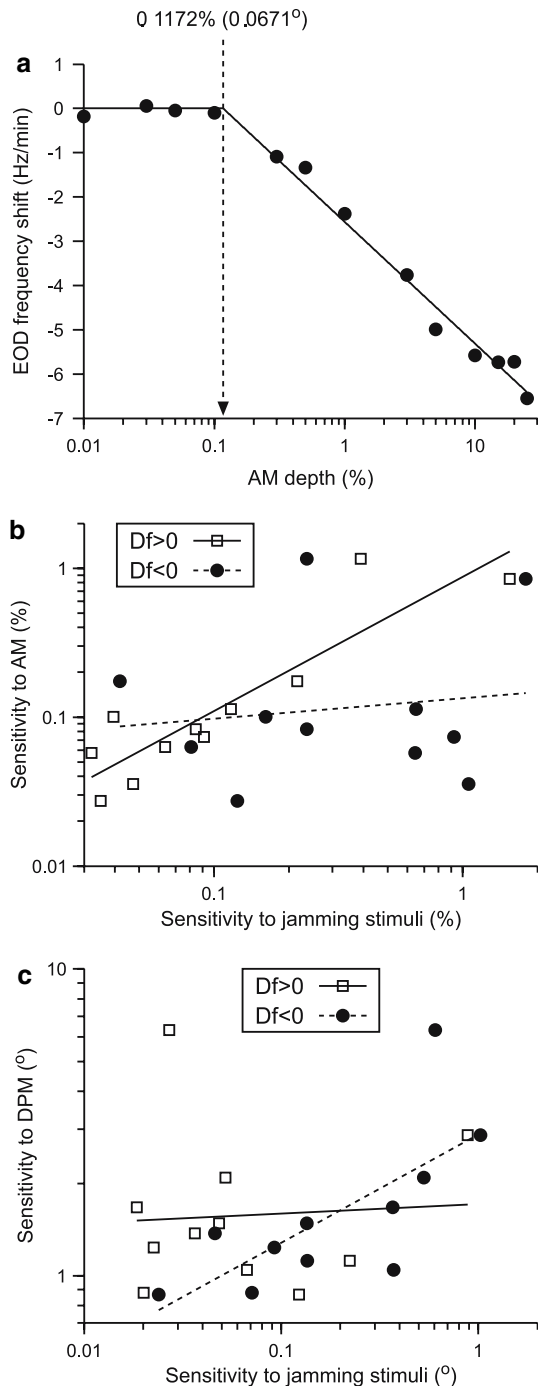


Fig. 6 Sensitivity to Df>0, Df<0, sinusoidal AM, and sinusoidal DPM in the phase chamber configuration. **a** Illustration of the method used to estimate sensitivity (see Methods for details). This example plots the shift in EOD frequency as a function of AM depth for the responses of one individual to Df>0 stimuli. The sensitivity (minimum AM depth that elicits a response) is estimated to be 0.1172%, which corresponds to 0.0671° of PM. **b** Correlations between sensitivity to sinusoidal AM and sensitivity to jamming stimuli (Df>0 and Df<0) across 11 individuals. **c** Correlations between sensitivity to sinusoidal DPM and sensitivity to jamming stimuli (Df>0 and Df<0) across the same 11 individuals

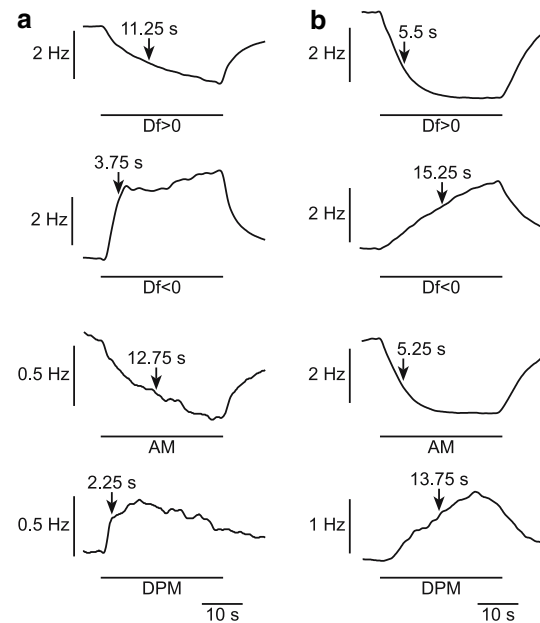


Fig. 7 Time course of responses to jamming and non-jamming stimuli presented in the phase chamber configuration. Average responses to three repeated presentations of Df>0, Df<0, AM, and DPM are shown for two different individuals in **(a)** and **(b)**. The bar beneath each average response represents the period of stimulus modulation. Arrows show the time constants of each of the average responses

the following values: $a = -8.5062^\circ$, $b = -0.5486^\circ$, $c = 1.2860^\circ$, and $d = 2.9617^\circ$ ($r^2 = 0.9941$, Fig. 8a); for variation in AM depth, the fit resulted in the following values: $a = -9.2328\%$, $b = 0.2584\%$, $c = 0.2144\%$, and $d = 3.1698\%$ ($r^2 = 0.9897$, Fig. 8b). The b -values from the two fits are particularly informative, as they reveal the extent to which the curves are shifted to the left or right of the y -axis, and therefore the depth of modulation and sense of rotation that approximates the perceptual transition between stimuli identified as Df>0 and Df<0, which in both cases deviates from 0. The leftward shift of the curve in Fig. 8a accounts for the decelerations in EOD frequency that are elicited by AM presented alone (PM depth = 0°, dashed line in Fig. 8a), whereas the rightward shift of the curve in Fig. 8b accounts for the accelerations in EOD frequency that are elicited by DPM presented alone (AM depth = 0%, dashed line in Fig. 8b).

Responses to AM stimuli

Presenting random AM under global stimulus conditions (i.e., Fig. 3a) elicited decelerations in EOD frequency of a magnitude similar to the decelerations caused by sinusoidal AM (Fig. 9a). However, these decelerations required frequency components below ~20 Hz within the random AM

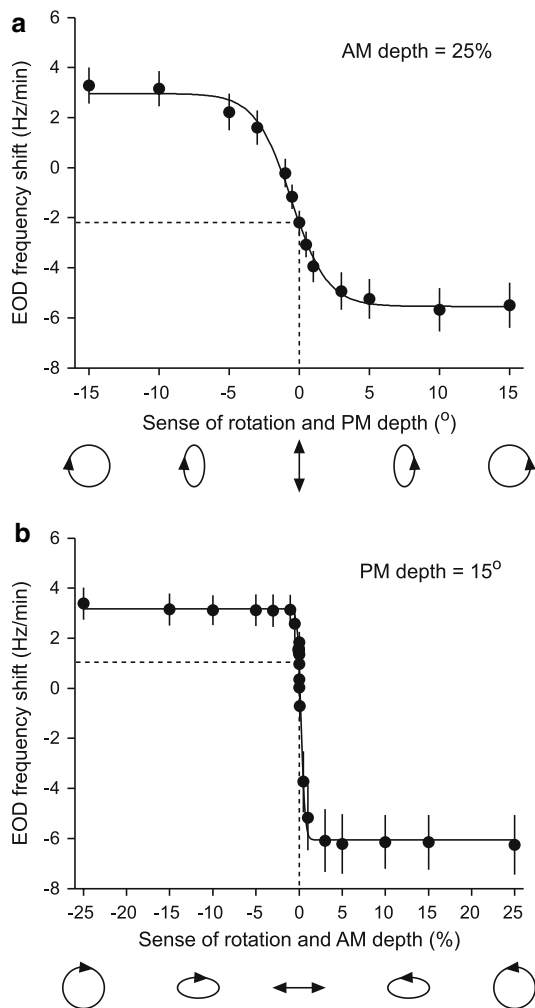


Fig. 8 Shifts in EOD frequency in response to varying depths of DPM with AM depth held constant at 25% (a), or varying depths of AM with DPM depth held constant at 15° (b). In both cases, Lissajous plots of the stimulus modulations are plotted below the abscissa, and the sense of rotation is reflected in the sign of the modulation depth, with *negative values* representing a clockwise rotation and *positive values* representing a counterclockwise rotation (modulation rate = 2 Hz in each case). In both cases the data are fit with a sigmoidal function and the responses to pure AM (DPM depth = 0°) and pure DPM (AM depth = 0%) are marked by *dashed lines*

(Fig. 9b). Thus, there was no significant difference in the magnitude of decelerations induced by random AM with frequency spectra ranging from 0 to 20 and from 0 to 100 Hz (Tukey HSD test, $n = 9$, and $P > 0.44$). However, the responses to both of these random AM stimuli were significantly greater in magnitude than the responses elicited by random AM with frequency spectra ranging from 30 to 100, 50 to 100, and 70 to 100 Hz (Tukey HSD test, $n = 9$, and $P < 0.01$).

Presenting both sinusoidal and random AM under local stimulus conditions (i.e., Fig. 3b) also reliably elicited

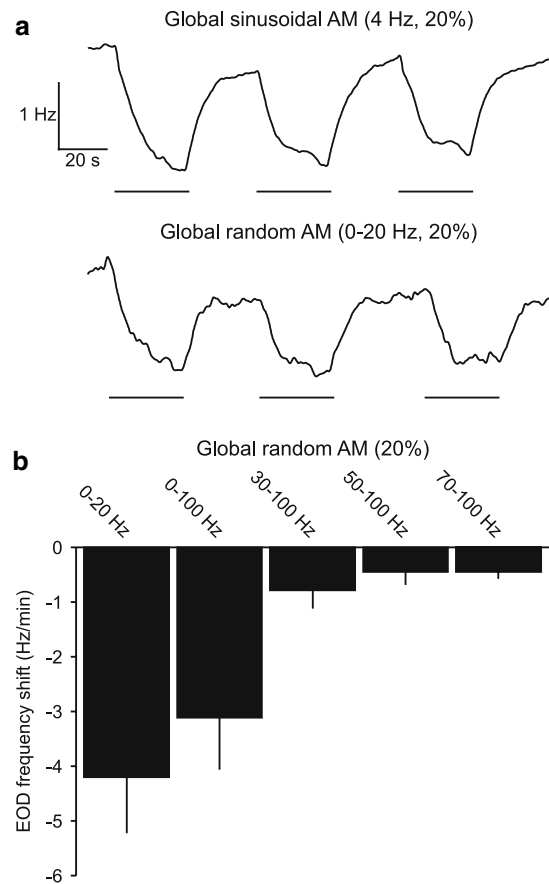


Fig. 9 Responses to global AM. **a** Responses of a single individual to three repeated presentations of sinusoidal AM at a depth of 20% and a modulation rate of 4 Hz and three repeated presentations of random AM at a depth of 20% and a frequency spectrum ranging from 0 to 20 Hz, both presented in the global stimulus configuration. The *bars* beneath each trace represent the periods of stimulus modulation. **b** Mean shift in EOD frequency (\pm SEM and $n = 9$ fish) in response to random AM stimuli with different frequency spectra presented in the global stimulus configuration

decreases in EOD frequency (Fig. 10a). EOD frequency shifts could usually be elicited by localized AM stimuli with depths $<5\%$ of the carrier amplitude as measured at the site of stimulation (Fig. 10b). Transient shifts ('ramps') in the carrier amplitude presented under global stimulus conditions (i.e., Fig. 3a) also resulted in weak, but consistent decreases in EOD frequency, with the magnitude of frequency decreases increasing with greater shifts in amplitude (Fig. 11).

Responses to moving resistive objects

Sinusoidally moving a plastic rod along the flank of the fish (i.e., Fig. 3c) at a rate of 1 Hz (average rate of motion of 10 cm/s, see Methods) caused modulations in the amplitude of the EOD replacement signal (Fig. 12a), as expected

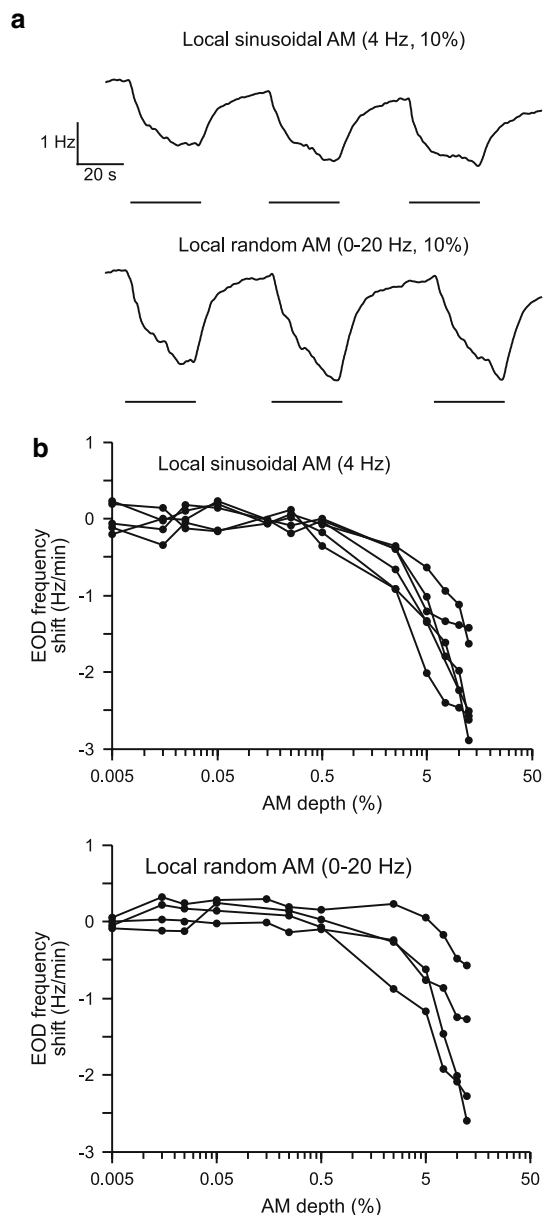


Fig. 10 Responses to local AM. **a** Responses of a single individual to three repeated presentations of sinusoidal AM at a depth of 10% and a modulation rate of 4 Hz and three repeated presentations of random AM at a depth of 10% and a frequency spectrum ranging from 0 to 20 Hz, both presented in the local stimulus configuration. The bars beneath each trace represent the periods of stimulus modulation. **b** Shifts in EOD frequency as a function of AM depth for local sinusoidal AM at a modulation rate of 4 Hz ($n = 6$ fish) and local random AM with a frequency spectrum ranging from 0 to 20 Hz ($n = 4$ fish)

for a resistive object. The amplitude of the signal reached a maximum directly adjacent to the object, as seen by a peak in amplitude when the object passed by the anode and a trough when it passed by the cathode of a pair of recording electrodes (Fig. 12a). We used rods of three different diameters: 6, 5, and 3 mm, which resulted in AM depths of

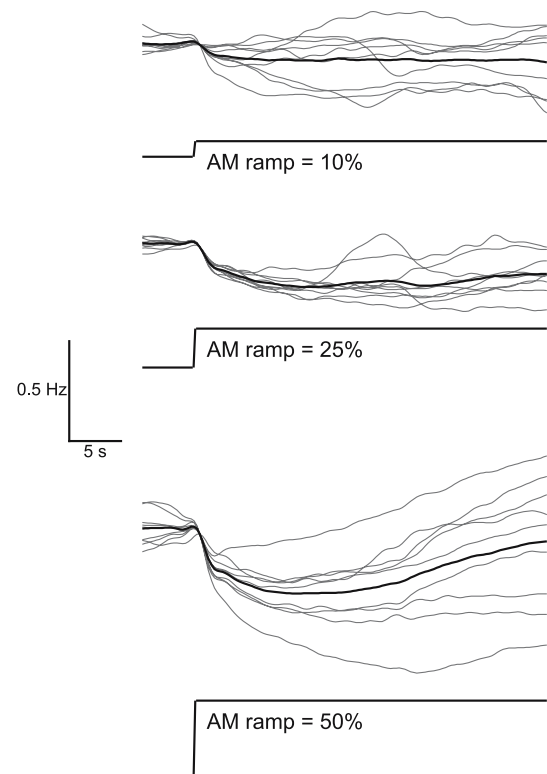


Fig. 11 Responses to upward amplitude ramps in a single individual in the global stimulus configuration. Responses to three different magnitudes of ramps are shown: 10, 25, and 50%, with nine separate responses to each magnitude plotted as *thin gray lines*, and the averages of each set of nine responses plotted as *thick black lines*. In each case, the upward ramp (illustrated below each set of responses) is linear with a duration of 250 ms

12.0, 10.9, and 4.3%, respectively (as measured from baseline to the peak).

Movement of the 6 and 5 mm diameter rods reliably elicited shifts in EOD frequency, whereas movement of the 3 mm diameter rod resulted in relatively weak, inconsistent responses. Typically, the responses to the larger diameter rods consisted of an immediate, transient rise in EOD frequency, followed by a stronger, maintained decrease in frequency (Fig. 12b). To verify that these responses resulted from modulations in the amplitude of the EOD replacement signal and not some other modality, we compared responses to object motion when the EOD replacement was turned off (no electrosensory stimulus) with those when it was turned on. In most cases, the early, transient rise in frequency still occurred when the EOD replacement was turned off, but the subsequent decrease in frequency was greatly attenuated (Fig. 12b). Nevertheless, a relatively weak frequency decrease still occurred in most cases when the EOD replacement was turned off (Fig. 12c). The decrease in EOD frequency was significantly greater when the EOD replacement was turned on

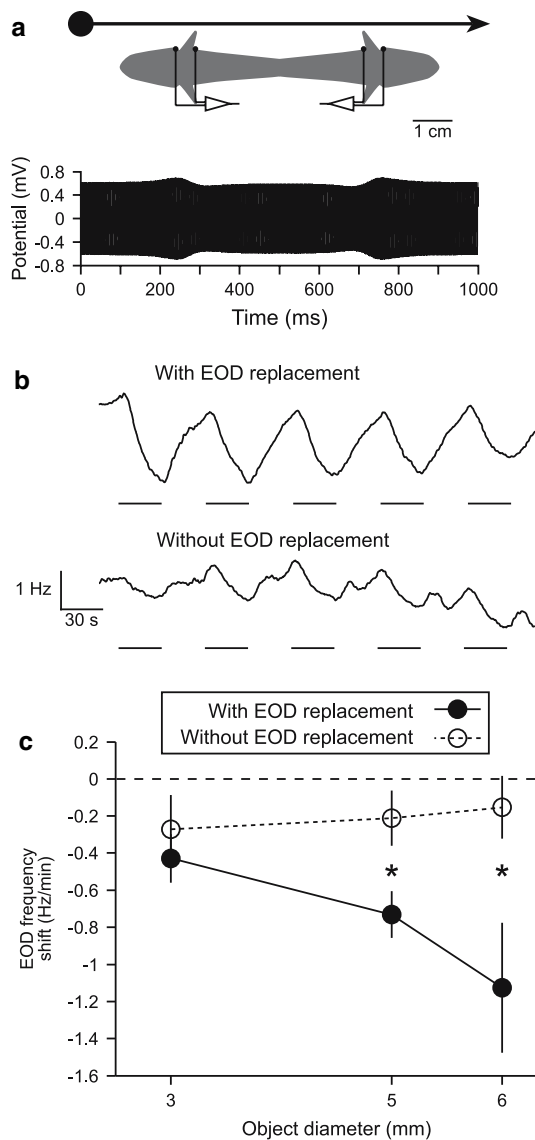


Fig. 12 Amplitude modulation resulting from a moving plastic rod causes decreases in EOD frequency. **a** Schematic diagram of a fish showing the motion of a moving plastic rod. A mirror image of the fish is shown to represent the cyclic nature of the rod's motion and the location of a pair of electrodes used to measure changes in the amplitude of the EOD replacement signal are shown (note that these measurements are actually made in the absence of the fish). Plot shows the modulation in potential resulting from the rod's motion. The abscissa is aligned with the schematic and scaled so that the time course of the modulated potential follows the location of the rod as it moves along the side of the fish. **b** Responses of a single individual to five repeated presentations of a 6 mm diameter moving plastic rod, with and without the EOD replacement signal. The bars beneath each trace represent the periods of stimulus modulation. **c** Mean shift in EOD frequency (\pm SEM and $n = 8$ fish) in response to moving plastic rods of three different diameters, with and without the EOD replacement. Significant differences, as determined by a Wilcoxon matched-pairs test, are noted by asterisks

than when it was turned off for the 6 and 5 mm diameter rods (Wilcoxon matched-pairs test, $n = 8$, and $P < 0.05$), but not for the 3 mm diameter rod ($P > 0.4$) (Fig. 12c).

Discussion

We recently showed that sinusoidal AM and sinusoidal DPM presented alone can elicit shifts in EOD frequency that are similar to JARs in a direction that is predicted by the responses of primary electrosensory afferents to these stimuli (Fig. 2) (Carlson and Kawasaki 2006). We therefore concluded that the responses to sinusoidal AM and sinusoidal DPM presented alone are behavioral responses that are driven by 'phantom' jamming signals created within the neuronal circuits that mediate the JAR. An alternative interpretation, however, is that these behaviors may be different from the JAR and may be mediated by distinct neuronal mechanisms that serve a different function. In the previous study, we provided support for the former interpretation by showing that responses to sinusoidal AM and sinusoidal DPM presented alone were greatly reduced when these sinusoidal modulations were accompanied by random modulation of the other stimulus attribute (i.e., sinusoidal AM with random DPM, or vice versa), a treatment that eliminates the responses of primary afferents to sinusoidal modulation of their non-preferred stimulus attribute (see Carlson and Kawasaki 2006 for details). The first objective of the current study was to further address this problem by quantifying behavioral responses to a variety of jamming and non-jamming stimuli to better assess their similarities and differences. The second objective was to determine whether EOD frequency shifts could be elicited by non-jamming stimuli that fish may encounter in their natural environment.

Asymmetries in jamming avoidance responses elicited by positive and negative frequency differences

Previous work using free-field stimulation in *Eigenmannia* demonstrated that JARs to $Df > 0$ are tuned to higher rates of modulation than JARs to $Df < 0$ (best rates: $Df > 0 = 3.34 \pm 0.3$ Hz, $Df < 0 = 2.56 \pm 0.14$ Hz, and $n = 20$ fish), but no significant difference was detected (Bastian and Yuthas 1984). Our results support this finding and reveal a significant difference in modulation rate tuning in both free-field and phase chamber stimulus configurations (Figs. 4, 5). The same earlier study demonstrated that responses to $Df > 0$ exhibited significantly greater time constants than responses to $Df < 0$ (Bastian and Yuthas 1984). Although we observed a trend in the same direction, the difference was not significant. We also found that the fish are more sensitive to $Df > 0$ than to $Df < 0$ (i.e., JARs to $Df > 0$ can be elicited by weaker stimuli than those required to elicit JARs to $Df < 0$). The overall sensitivity we measured is similar to previously reported values based on different methods to assess responses to alternating presentation of $Df > 0$ and $Df < 0$ (Rose and Heiligenberg 1985;

Carr et al. 1986a; Kawasaki 1997). The results of our study and the previous study by Bastian and Yuthas (1984) clearly reveal that behavioral responses to $Df > 0$ and $Df < 0$ show systematic asymmetries in terms of modulation rate tuning, sensitivity, and possibly time course. Sex differences and asymmetries in the JAR on an individual level have previously been reported using freely behaving fish with natural EODs (Kramer 1987, 1999). It would be interesting to determine both the functional significance of these asymmetries in the JAR, as well as their neuronal basis, i.e., where in the JAR pathway they arise. Sign-selective neurons in the thalamic nucleus electrosensorius, which receive input from midbrain electrosensory neurons and project to prepacemaker regions that mediate EOD frequency shifts, were previously shown to exhibit an asymmetry in modulation rate tuning in the same direction as the behavioral asymmetry we describe: $Df > 0$ -selective neurons were tuned to an average modulation rate of 4.9 ± 0.66 Hz ($n = 7$ neurons), whereas $Df < 0$ -selective neurons were tuned to an average modulation rate of 3.6 ± 0.56 Hz ($n = 4$ neurons) (Bastian and Yuthas 1984). This difference was not significant, but this could be due to the low-sample size. To our knowledge, other differences in the response properties of sign-selective neurons within the nucleus electrosensorius or other regions, such as the midbrain, have not been described.

Similarities between JARs and responses to non-jamming stimuli

We found that behavioral responses to sinusoidal AM are similar to JARs to $Df > 0$, whereas behavioral responses to sinusoidal DPM are similar to JARs to $Df < 0$, in terms of tuning to modulation rate (Figs. 4, 5), sensitivity (Fig. 6), and the time course of responses (Fig. 7). Behavioral responses to sinusoidal AM were greatest at modulation rates of 2–4 Hz, similar to JARs to $Df > 0$, whereas behavioral responses to sinusoidal DPM were greatest at modulation rates of 1–2 Hz, similar to JARs to $Df < 0$. Furthermore, frequency decreases could be elicited by random AM, but only if the frequency spectrum of random modulations contained energy within the low frequencies that elicit normal JARs (Fig. 9). In addition, individual differences in sensitivity to sinusoidal AM were correlated with individual differences in sensitivity to $Df > 0$, but not $Df < 0$, whereas the reverse was true for individual differences in sensitivity to sinusoidal DPM. Similarly, individual differences in the time course of responses to sinusoidal AM were correlated with individual differences in the time course of responses to $Df > 0$, but not $Df < 0$, whereas the reverse was true for individual differences in the time course of responses to sinusoidal DPM. Together, these findings lend strong support to the hypothesis that the re-

sponses to sinusoidal AM and sinusoidal DPM presented alone are responses to ‘phantom’ jamming stimuli, i.e., that sinusoidal AM is mistakenly perceived as $Df > 0$ and sinusoidal DPM is mistakenly perceived as $Df < 0$ (Carlson and Kawasaki 2006).

By systematically varying the depth of sinusoidal AM or sinusoidal DPM while maintaining the temporal relationships that occur between them during actual jamming, we found that changes in EOD frequency could be fit as a smooth, sigmoidal function of variation in the relative depths of AM and DPM (Fig. 8). This smooth transition provides further support for the conclusion that the responses to sinusoidal AM and sinusoidal DPM presented alone do not represent distinct behaviors, but relate to the position of these stimuli along a perceptual continuum that includes the JAR. This kind of response function, with two plateaus separated by a smooth, but sharp transition between them, is characteristic of behavioral responses to stimuli that are perceived categorically (Ehret 1987; Wytenbach and Hoy 1999), in this case as either $Df > 0$ or $Df < 0$. If these stimuli were accurately perceived, then the midpoint of the transition between the two plateaus would occur at a value of 0° in Fig. 8a (no DPM) and 0% in Fig. 8b (no AM), as these values represent the actual boundaries between stimuli that have a $Df > 0$ -characteristic temporal relationship between AM and DPM and stimuli that have a $Df < 0$ -characteristic temporal relationship between AM and DPM. However, the curve in Fig. 8a is shifted to the left by 0.5486° , which represents the actual amount of PM that is required to compensate for the AM-induced phantom PMs of T-afferents. Similarly, the curve in Fig. 8b is shifted to the right by 0.2584% , which represents the actual amount of AM that is required to compensate for the PM-induced phantom AMs of P-afferents (Carlson and Kawasaki 2006).

These various lines of evidence all suggest that the shifts in EOD frequency caused by non-jamming stimuli arise from the phantom modulations of primary electrosensory afferents, and are mediated by the same neuronal pathway serving the JAR. However, our evidence is correlational, and it remains a possibility that either the amplitude- or time-coding pathways directly activate pre-motor elements of the JAR circuitry. Definitively testing this possibility will require independent stimulation of the two pathways, which is not feasible using electrosensory stimuli. However, it may be possible to achieve this manipulation through microstimulation of specific electrosensory regions of the brain, such as the preeminent nucleus.

A related problem is that the JAR relies on timing differences between different locations on the body surface (Heiligenberg et al. 1978; Heiligenberg and Rose 1985; Carr et al. 1986a, b). If EOD frequency decreases in response to AM are truly caused by phantom PMs, then there

must be a timing reference for detecting differences in T-afferent spike times at different points on the body surface (Takizawa et al. 1999). In the phase chamber configuration, the reference is the unmodulated compartment. For localized stimuli, such as the moving object or localized AM stimulation, the body surfaces removed from the site of stimulation serve as a timing reference. The nature of the timing reference for global AM is not as clear. Different P- and T-afferents exhibit different degrees of sensitivity to AM (Carlson and Kawasaki 2006). Apparently, this difference is partly caused by the uneven geometry of the EOD replacement signal, in that different portions of the body surface receive different field strengths. Under this scenario, T-afferents that respond more strongly to AM would be on the same location on the body surface as P-afferents that respond more strongly to AM. Because the JAR favors the pattern of stimulation that occurs at the most strongly modulated points on the body surface (Heiligenberg et al. 1978), the location where both P- and T-afferents are relatively weakly modulated would serve as a timing reference. Definitively testing this hypothesis would require eliminating all phantom phase differences at all locations on the body surface, a manipulation that may be impossible to achieve in practice.

Phantom jamming stimuli in a natural context

Although our results strongly suggest that EOD frequency shifts can be elicited by phantom jamming stimuli, an important question is whether these effects have any functional significance on electrosensory processing and perception. This general question can be divided into two separate lines of inquiry: first, whether stimuli that the fish encounter in their natural environment can act as phantom jamming stimuli; and second, since the fish are using an active sensing system, whether such frequency shifts, in turn, have any effect on electrosensory processing and perception. One goal of the current study was to directly address the former question by presenting fish with semi-natural stimuli and assessing the resulting changes in EOD frequency. In general, the fish responded to any semi-natural stimulus that resulted in AM by decreasing their EOD frequency, including random AM (Figs. 9, 10), similar to what would occur if a fish swam through a dense, highly structured environment (Crampton 1998); highly localized AM (Fig. 10), as would occur if a small prey item entered a fish's electric field (Nelson and MacIver 1999; Nelson et al. 2002; Chacron et al. 2003); transient changes in amplitude (Fig. 11), as would occur if a fish crossed the boundary between two bodies of water with differing conductivity, such as a fresh rainwater flow or the confluence of two streams or rivers (Hopkins 1999); and finally, actual moving resistive objects (Fig. 12). An earlier study in

Eigenmannia revealed that moving objects with complex impedances can elicit shifts in EOD frequency (Rose and Heiligenberg 1986). Because those objects had both resistive and capacitive components, the direction of frequency shifts was related to the relationship between actual modulations in the amplitude and phase of the electric field, as is the case for natural JARs. We show for the first time that such shifts can be elicited by purely resistive objects as well, presumably due to the phantom PMs they generate in T-afferents. It therefore seems likely that fish would frequently encounter non-jamming stimuli in their natural environment that would elicit shifts in EOD frequency.

Phantom modulations and active electrolocation

It is important to note that our findings are only relevant in the context of one particular behavior, the JAR. It remains to be seen whether ambiguity at the level of individual primary afferents affects electrosensory processing as it relates to behaviors other than the JAR, most notably active electrolocation. In the context of active electrolocation, AM and PM result from the resistive and capacitive components of objects, respectively (von der Emde 1999), and a lack of independence in the encoding of these two attributes may prevent the fish from obtaining unambiguous information about the resistive and capacitive properties of objects. However, *Eigenmannia* can discriminate purely resistive objects from objects with capacitance (von der Emde 1998). It may be that ambiguity about AM and PM is resolved in central electrosensory pathways that are devoted to active electrolocation, but not for the JAR. Also, the effects of this ambiguity may be small enough that they simply do not affect the ability to distinguish these two features of objects. It would be interesting to use conditioning to test the fish's ability to unambiguously distinguish between modulations in the amplitude and phase of electrosensory stimuli. On the other hand, the responses of primary afferents to their non-preferred stimulus feature could actually enhance active electrolocation performance (Chacron 2007). For example, AM-induced shifts in the spike times of T-afferents could increase the amount of information about AM made available to the fish, since P- and T-afferents have different firing patterns, differences in frequency tuning, and different degrees of sensitivity (Scheich et al. 1973; Hopkins 1976; Zakon 1986).

The question of whether EOD frequency shifts in response to phantom jamming stimuli have any effect on electrosensory processing is completely open. Studies on the responses of central electrosensory neurons to stimulus modulations generally set the carrier frequency at a fixed value, as in the current behavioral study, or allow the carrier frequency to follow the fish's own pacemaker, without monitoring its relationship to electrosensory

responses. However, because the fish's electrosensory system is an active one, shifts in the EOD frequency will cause the fish to receive stimulus modulations at a different carrier frequency. It is unknown whether the responses of central electrosensory neurons to AM, PM, or actual objects would change during or following shifts in the carrier frequency. Primary afferents, especially T-afferents, tend to be sharply tuned, though they will generally continue to fire reliably if the frequency changes by only a few Hz and the amplitude remains in the normal behavioral range (Hopkins 1976; Zakon 1986). Nevertheless, small changes in carrier frequency could have slight, but detectable effects on central electrosensory responses, due either to the effects of peripheral tuning or central sensory processing. Such effects, if found, would not necessarily be maladaptive. In fact, central electrosensory neurons could be selectively tuned so that they respond more strongly to modulations in the electric field that occur during shifts in the EOD carrier frequency.

In addition, shifting the EOD frequency could provide fish with additional information. Objects with capacitance, such as live prey items, give rise to impedances and phase shifts that vary as a function of carrier frequency (von der Emde and Ringer 1992; Nelson et al. 2002). By shifting EOD frequency, then, the fish may be able to improve the signal-to-noise ratio of object-induced modulations and thereby enhance the identification and localization of encountered objects. Previous authors have noted a trade-off in the benefits to pulse-type and wave-type EODs, with pulse-type EODs conferring better spatial resolution due to their broad frequency content, and wave-type EODs conferring better temporal resolution due to their high-repetition rate (Scheich and Bullock 1974; Crampton 1998). Shifting the EOD frequency upon encountering an object may be a strategy for somewhat mitigating this tradeoff and improving spatial resolution. EOD frequency decreases in response to AM may therefore not simply be a byproduct of the JAR, but an adaptive response to improve electrolocation performance. In this regard, the responses to moving plastic rods are especially interesting (Fig. 12). Rather than a purely decelerating response, as observed in the responses to AM, fish responded to object motion by first slightly accelerating their EOD rate, and then decelerating it. Even when the EOD replacement was removed, this transient acceleration and a reduced deceleration were still present, indicating that other modalities, such as the mechanosensory lateral line, may play a role in mediating EOD frequency shifts, which would support an adaptive function in active electrolocation. These questions can be fruitfully explored using electrophysiological, behavioral, and computational approaches. In this regard, it is interesting that the related wave-type weakly electric fish *Sternopygus* does not produce JARs or similar types of

gradual EOD frequency shifts (Rose et al. 1987). This would seem to suggest that the EOD frequency shifts induced by phantom jamming stimuli in *Eigenmannia* do not serve an adaptive function, but are simply a byproduct of JAR evolution. On the other hand, the JAR may simply have represented an evolutionary precursor that set the stage for adaptive frequency shifts in the context of electrolocation. From this perspective, frequency shifts that were elicited by phantom jamming stimuli were not selected against because they actually turned out to be useful. Finally, a likely possibility is that such frequency shifts were simply not selected against because their effects are neutral in the context of electrolocation.

Our findings provide direct insight into the relationship between sensory perception and the information processing characteristics of individual neurons, a relationship that is often difficult to quantify in more complex sensory systems. Although the behavioral effects we describe are slight and may not have any significant effect on fitness, they are a stark reminder that sensory perception, for all animals, is not necessarily a direct reflection of the outside world. Instead, perception is an internal model that represents only enough information, and only to the requisite degree of accuracy, to perform a given behavior.

Acknowledgments This work was supported by grants from the National Institute of Neurological Disorders and Stroke (F32 NS049788 to B.A.C.) and the National Science Foundation (IBN-0235533 to M.K.). These experiments comply with the "Principles of animal care," publication No. 86-23, revised 1985 of the National Institutes of Health, and were approved by the University of Virginia Institutional Animal Care and Use Committee.

References

- Bastian J, Chacron MJ, Maler L (2002) Receptive field organization determines pyramidal cell stimulus-encoding capability and spatial stimulus selectivity. *J Neurosci* 22:4577–4590
- Bastian J, Yuthas J (1984) The jamming avoidance response of *Eigenmannia*: properties of a diencephalic link between sensory processing and motor output. *J Comp Physiol A* 154:895–908
- Bullock TH, Hamstra RH, Scheich H (1972a) The jamming avoidance response of high frequency electric fish. I. General features. *J Comp Physiol* 77:1–22
- Bullock TH, Scheich H, Hamstra RH (1972b) The jamming avoidance response of high frequency electric fish. II. Quantitative aspects. *J Comp Physiol* 77:23–48
- Carlson BA (2006) A neuroethology of electrocommunication: senders, receivers, and everything in between. In: Ladich F, Collin SP, Moller P, Kapoor BG (eds) Fish communication. Science Publishers, Enfield, NH, pp 805–848
- Carlson BA, Kawasaki M (2006) Ambiguous encoding of stimuli by primary sensory afferents causes a lack of independence in the perception of multiple stimulus attributes. *J Neurosci* 26:9173–9183
- Carr CE, Heiligenberg W, Rose GJ (1986a) A time-comparison circuit in the electric fish *Eigenmannia* midbrain I. Behavior and physiology. *J Neurosci* 6:107–119

- Carr CE, Maler L, Taylor B (1986b) A time-comparison circuit in the electric fish *Eigenmannia* midbrain II. Functional morphology. *J Neurosci* 6:1372–1383
- Chacron M (2007) Electrolocation. Scholarpedia, p 6776
- Chacron M, Doiron B, Maler L, Longtin A, Bastian J (2003) Non-classical receptive field mediates switch in a sensory neuron's frequency tuning. *Nature* 423:77–81
- Crampton W (1998) Electric signal design and habitat preferences in a species rich assemblage of gymnotiform fishes from the upper Amazon basin. *An Acad Bras Cienc* 70:805–847
- Ehret G (1987) Categorical perception of sound signals: facts and hypotheses from animal studies. In: Harnad S (eds) *Categorical perception: the groundwork of cognition*. Cambridge University Press, New York, pp 301–331
- Hagedorn M, Heiligenberg W (1985) Court and spark: electric signals in the courtship and mating of gymnotoid fish. *Anim Behav* 33:254–265
- Heiligenberg W (1973) Electrolocation of objects in the electric fish *Eigenmannia* (Rhamphichthyidae, Gymnotoidei). *J Comp Physiol* 87:137–164
- Heiligenberg W (1991) *Neural nets in electric fish*. MIT, Cambridge
- Heiligenberg W, Baker C, Matsubara J (1978) The jamming avoidance response in *Eigenmannia* revisited: the structure of a neuronal democracy. *J Comp Physiol* 127:267–286
- Heiligenberg W, Bastian J (1980) The control of *Eigenmannia*'s pacemaker by distributed evaluation of electroreceptive afferences. *J Comp Physiol* 136:113–133
- Heiligenberg W, Partridge BL (1981) How electroreceptors encode JAR-eliciting stimulus regimes: reading trajectories in a phase-amplitude plane. *J Comp Physiol* 142:295–308
- Heiligenberg WF, Rose G (1985) Phase and amplitude computations in the midbrain of an electric fish: intracellular studies of neurons participating in the jamming avoidance response of *Eigenmannia*. *J Neurosci* 5:515–531
- Hopkins C (1972) Sex differences in electric signaling in an electric fish. *Science* 176:1035–1037
- Hopkins C (1974) Electric communication: functions in the social behavior of *Eigenmannia virescens*. *Behaviour* 50:270–305
- Hopkins CD (1976) Stimulus filtering and electroreception: tuberosus electroreceptors in three species of gymnotoid fish. *J Comp Physiol* 111:171–207
- Hopkins CD (1999) Design features for electric communication. *J Exp Biol* 202:1217–1228
- Kawasaki M (1997) Sensory hyperacuity in the jamming avoidance response of weakly electric fish. *Curr Opin Neurobiol* 7:473–479
- Kramer B (1987) The sexually dimorphic jamming avoidance response in the electric fish *Eigenmannia* (Teleostei, Gymnotiformes). *J Exp Biol* 130:39–62
- Kramer B (1999) Waveform discrimination, phase sensitivity and jamming avoidance in a wave-type electric fish. *J Exp Biol* 202:1387–1398
- Nelson ME, MacIver MA (1999) Prey capture in the weakly electric fish *Apteronotus albifrons*: sensory acquisition strategies and electrosensory consequences. *J Exp Biol* 202:1195–1203
- Nelson ME, MacIver MA, Coombs S (2002) Modeling electrosensory and mechanosensory images during the predatory behavior of weakly electric fish. *Brain Behav Evol* 59:199–210
- Ramcharitar J, Tan E, Fortune E (2005) Effects of global electrosensory signals on motion processing in the midbrain of *Eigenmannia*. *J Comp Physiol A* 191:865–872
- Rose G, Heiligenberg W (1985) Temporal hyperacuity in the electric sense of fish. *Nature* 318:178–180
- Rose GJ, Heiligenberg W (1986) Neural coding of difference frequencies in the midbrain of the electric fish *Eigenmannia*: reading the sense of rotation in an amplitude-phase plane. *J Comp Physiol A* 158:613–624
- Rose GJ, Keller C, Heiligenberg W (1987) 'Ancestral' neural mechanisms of electrolocation suggest a substrate for the evolution of the jamming avoidance response. *J Comp Physiol A* 160:491–500
- Scheich H, Bullock TH, Hamstra RH (1973) Coding properties of two classes of afferent nerve fibers: high frequency electroreceptors in the electric fish, *Eigenmannia*. *J Neurophysiol* 36:39–60
- Scheich J, Bullock TH (1974) The detection of fields from electric organs. In: Fessard A (ed) *Handbook of sensory physiology*. Springer, New York, pp 201–256
- Takizawa Y, Rose GJ, Kawasaki M (1999) Resolving competing theories for control of the jamming avoidance response: the role of amplitude modulations in electric organ discharge decelerations. *J Exp Biol* 202:1377–1386
- von der Emde G (1998) Capacitance detection in the wave-type electric fish *Eigenmannia* during active electrolocation. *J Comp Physiol A* 182:217–224
- von der Emde G (1999) Active electrolocation of objects in weakly electric fish. *J Exp Biol* 202:1205–1215
- von der Emde G, Ringer T (1992) Electrolocation of capacitive objects in four species of pulse-type weakly electric fish. I. Discrimination performance. *Ethology* 91:326–338
- Watanabe A, Takeda K (1963) The change of discharge frequency by A.C. stimulus in a weakly electric fish. *J Exp Biol* 40:57–66
- Wyttenbach RA, Hoy RR (1999) Categorical perception of behaviorally-relevant stimuli by crickets. In: Hauser MD, Konishi M (eds) *The design of animal communication*. MIT, Cambridge, MA, pp 559–576
- Zakon HH (1986) The electroreceptive periphery. In: Bullock TH, Heiligenberg W (eds) *Electroreception*. Wiley, New York, pp 103–156